ChemComm

COMMUNICATION

View Article Online
View Journal | View Issue

Cite this: *Chem. Commun.*, 2025, **61**, 3540

Received 29th July 2024,
Accepted 20th November 2024

DOI: 10.1039/d4cc03807j

rsc.li/chemcomm

Deuterated oxazines are bright near-infrared fluorophores for mitochondrial imaging and single molecule spectroscopy†

Blaise Gatin-Fraudet, *[a] Julius Seifert,[a] Kris Sarach,[a] Christina Holmboe Olesen, [a] Ramona Birke,[a] Sigrid Milles, [a] Melissa Birol,[b] Martin Lehmann[a] and Johannes Broichhagen *[a]

Bright near-infrared fluorophores are in demand for microscopy. We showcase a deuterated oxazine being 23% brighter *vs.* ATTO700. With a longer lifetime of 1.85 nanoseconds, we find the best-in-class SulfoOxazine700-d10 to stain mitochondria for confocal microscopy, and demonstrate unaffected diffusion properties in single molecule fluorescence correlation spectroscopy.

Fluorescence is a fascinating phenomenon that has changed the life science to observe cellular structures and to measure biomolecule behaviour on the single molecule level. The observed fluorophore comes with important parameters, such as its excitation and emission wavelengths, its absorptivity, fluorescence quantum yield and lifetime. Dyes in the near-infrared region are particularly interesting,[1] since less autofluorescence is present in this regime, and light of longer wavelengths penetrates tissues deeper. As such, they have gathered increasing interest in photodynamic therapy,[2] biological imaging,[3,4] protein labelling,[5] and material science.[6] However, they still suffer from poorer brightness and shorter lifetimes. Given our recent exploration of ATTO700-one of the best performing molecules in the NIR range in Förster resonance energy transfer (FRET) and stimulated emission by depletion (STED) microscopy,[7] we aimed to improve this oxazine dye. One strategy that has proven highly successful is the replacement of carbon-hydrogen (CH) by carbon deuterium (CD). This approach has entered chemical biology to augment rhodamine[8,9] and cyanine fluorophores,[10] as well as azobenzene photoswitches[11] for photopharmacology and has furthermore found applications for increasing stability in organic light emitting diodes.[12] A big advantage of this method is its minimal impact on the structure, and that one may use existing synthetic pathways, instead of *de novo* design and synthesis. Another benefit is that excitation and emission wavelengths do not change by this approach, making predictions about fluorescence behaviour solid.

In this study, we set out to improve ATTO700 based on a report by Pauff *et al.*,[13] to first synthesize oxazine scaffolds in order to obtain insight as to whether this strategy works on these molecular structures and by adding a sulfonate, installing a negative charge for water solubility (Fig. 1A). Commencing with *m*-anisidine (**1**) in an Ytterbium(III) catalyzed reaction with acetone, we obtained dihydroquinoline **2** in 65% yield, which was alkylated using ethyl iodide or ethyl bromide-d5 to access **3a** and **3b**, respectively (62% and 46% yield) (Fig. 1B). Sulfonation on the allylic methyl position was achieved using oleum in aqueous sulfuric acid, giving access to **4a** and **4b** in 67% and 66% yield, respectively. We designed the synthesis for a mix and match strategy to build oxazines with varying deuteration and sulfonation patterns. To do so, **3** and **4** were converted to four *para*-nitro azobenzenes **5** using the stable and storable 4-nitrobenzenediazonium tetrafluoroborate salt in a mixture of methanol and aqueous H_2SO_4 in moderate to excellent yields (**5a**: 82%; **5b**: 78%; **5c**: 93%; **5d**: 65%) by precipitation, in sufficient purity, neglecting the need for further purification. In parallel, **3** was demethylated to the dihydroquinoline-7-ol using BBr_3 in 73% and 80% yield for the non-deuterated and deuterated version **6a** and **6b**, respectively. We then were able to build oxazine700 derivatives with varying degrees of ethyl group deuteration: **Oxazine700-d0** (**5a** + **6a**; 32% yield), **Oxazine700-d5** (**5b** + **6a**; 24% yield), and **Oxazine700-d10** (**5b** + **6b**; 6% yield) (Fig. 1B). We noticed that this reaction was challenging, and equally successful using purified or crude **6**, so the notable drop in isolated yield may stem either from the kinetic isotope effect, or from less pure **6b** compared to **6a**. With these compounds in hand, we were able to determine key

[a] *Leibniz-Forschungsinstitut für Molekulare Pharmakologie, Robert-Rössle-Str. 10, 13125 Berlin, Germany*
E-mail: gatinfraudet@fmp-berlin.de, broichhagen@fmp-berlin.de
[b] *Berlin Institute of Medical Systems Biology (BIMSB), Max Delbrück Center for Molecular Medicine, Hannoversche Str. 28, 10115 Berlin, Germany*

† Electronic supplementary information (ESI) available: Chemical synthesis and characterization; details of photophysical characterization and cell culture; Fig. S1. See DOI: https://doi.org/10.1039/d4cc03807j

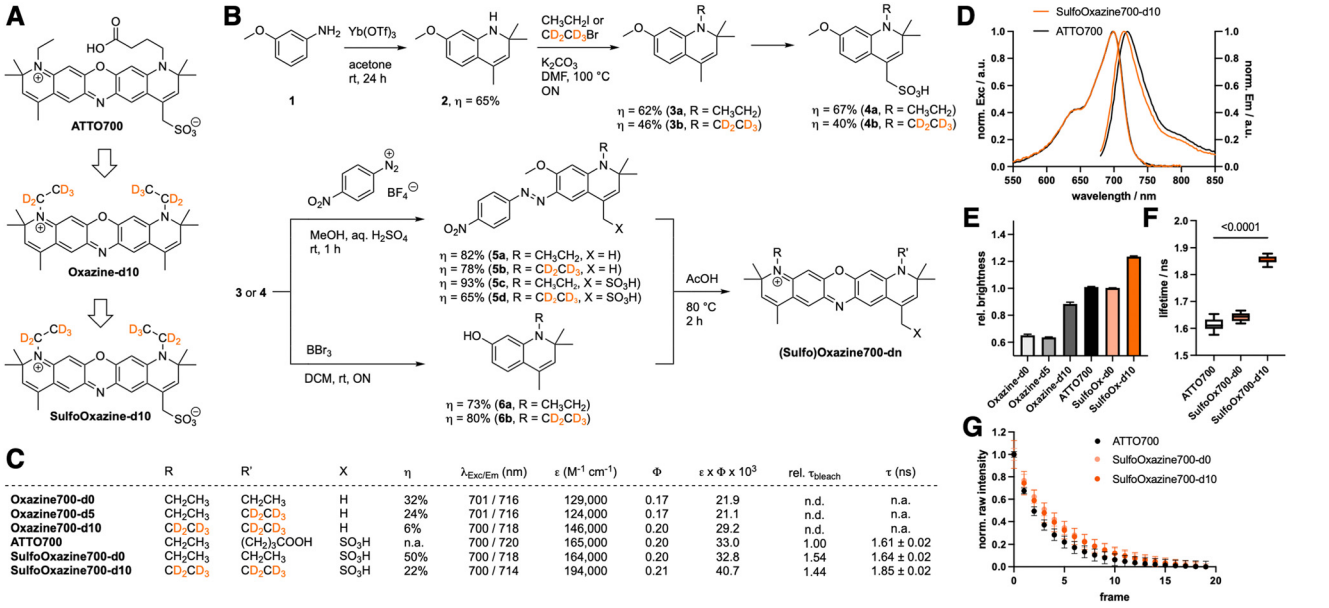

C

	R	R'	X	η	$\lambda_{Exc/Em}$ (nm)	ε (M^{-1} cm^{-1})	Φ	ε x Φ x 10^3	rel. τ_{bleach}	τ (ns)
Oxazine700-d0	CH_2CH_3	CH_2CH_3	H	32%	701 / 716	129,000	0.17	21.9	n.d.	n.a.
Oxazine700-d5	CH_2CH_3	CD_2CD_3	H	24%	701 / 716	124,000	0.17	21.1	n.d.	n.a.
Oxazine700-d10	CD_2CD_3	CD_2CD_3	H	6%	700 / 718	146,000	0.20	29.2	n.d.	n.a.
ATTO700	CH_2CH_3	$(CH_2)_3COOH$	SO_3H	n.a.	700 / 720	165,000	0.20	33.0	1.00	1.61 ± 0.02
SulfoOxazine700-d0	CH_2CH_3	CH_2CH_3	SO_3H	50%	700 / 718	164,000	0.20	32.8	1.54	1.64 ± 0.02
SulfoOxazine700-d10	CD_2CD_3	CD_2CD_3	SO_3H	22%	700 / 714	194,000	0.21	40.7	1.44	1.85 ± 0.02

Fig. 1 Approach, synthesis and characterization of deuterated oxazines. (A) The deuteration strategy exemplified on the ATTO700 oxazine backbone. (B) Synthetic scheme to yield five different oxazines in total: each non-, half- and fully ethyl group deuterated oxazine (Oxazine700-d0/d5/d10) scaffold and non- and fully deuterated sulfonated oxazine (SulfoOxazine700-d0/d10). (C) Photophysical and chemical properties of oxazines, the latter relative to ATTO700. Chemical yields are reported for the last synthetic step. Replicates: molar extinction coefficient: n = 3; fluorescence excitation and emission maximal wavelengths; quantum yield: n = 4; brightness; fluorescence lifetime: n = 12; photobleaching: n = 3. n.d. = not determined; n.a. = not available. (D) Normalized excitation and emission spectra of ATTO700 (black) and SulfoOxazine700-d10 (orange) in PBS. (E) Brightness of (Sulfo)Oxazine700-d0/10 relative to ATTO700. Mean ± SD from duplicate measures of excitation coefficient and triplicate measurements of quantum yield. (F) Fluorescence lifetimes of (Sulfo)Oxazine700-d0/10 and ATTO700 in PBS. λ_{Exc} = 640 nm; λ_{Em} = 690–784 nm. Multiple unpaired t-tests. Min to max box and whiskers, n = 12. (G) Bleaching analysis of (Sulfo)Oxazine700-d0/10 and ATTO700 in PBS. λ_{Exc} = 640 nm; λ_{Em} = 690–784 nm. Mean ± SD, n = 3.

photophysical properties, *i.e.* maxima of excitation and emission wavelength, molar extinction coefficient, and quantum yield. While the excitation and emission profiles in PBS were quite similar ($\lambda_{Exc/Em}$ in nm: **Oxazine700-d0**: 701/716; **Oxazine700-d5**: 701/716; **Oxazine700-d10**: 700/718) (Fig. 1B), we observed a remarkable increase in extinction and quantum yield for **Oxazine700-d10** compared to the non- or half-deuterated species in PBS (ε in M^{-1} cm^{-1} and Φ: **Oxazine700-d0:** 129 000 and 0.17; **Oxazine700-d5**: 124 000 and 0.17; **Oxazine700-d10:** 146 000 and 0.20) (Fig. 1C). The observation that half-deuteration does not show any improvements leads us to the suggestion that one non-deuterated ethyl group is sufficient for vibrational, non-radiative decays, supported by the timescale such processes occur ($\tau_{vibr} \sim 10^{-12}$ s; $\tau_{fluo} \sim 10^{-9}$ s). Our efforts to obtain lifetimes on a confocal microscope equipped with a FLIM module were unsuccessful since the dyes seemed to form aggregates on the solvent boundaries in the small volumes used. We then compared the small oxazine library to commercially available **ATTO700**, for which ε and Φ were reported to be 125 000 M^{-1} cm^{-1} and 0.25 (ref. 14), respectively. We assessed these parameters in-house, and found ε and Φ to be 165 000 M^{-1} cm^{-1} and 0.20, respectively. As we measured higher extinction yet lower quantum yield, the absolute brightness is comparable with a value of 33.0, that we report here (Fig. 1C). As such, **ATTO700** performed better than the oxazines. However, and importantly, the improving trend of deuteration from d0 to d5 to d10 stayed promising. In addition, sulfonation on dyes is reported to increase brightness[15] and such a moiety is present on **ATTO700**. Accordingly, we next set out to synthesize **SulfoOxazine700-d0** and **SulfoOxazine700-d10** (consciously neglecting the half-deuterated compound since no or less improvement was observed with oxazines) by using **5c, d** in a reaction with **6a, b.** Interestingly, the isolated yields were much higher compared to the non-sulfonated versions (50% and 22%). With these in hand, we pursued with characterization, and while λ_{Exc} = 700 nm remained constant, a small hypsochromic shift by 6 nm was observed for **SulfoOxazine700-d10** (Fig. 1C and D). Gratifyingly, while **SulfoOxazine700-d0** was close to **ATTO700**, we recorded an increase in extinction and quantum yield for **SulfoOxazine700-d10** with 194 000 M^{-1} cm^{-1} and 0.21, respectively, resulting in a total increase in brightness of 23% (Fig. 1B and E). Fluorescence lifetime of **SulfoOxazine700-d10** was also significantly increased by 15% at 100 nM in PBS, with τ = 1.85 ns ($\tau_{ATTO700}$ = 1.61 ns and $\tau_{SulfoOxazine700\text{-}d0}$ = 1.64 ns) (Fig. 1B and F). Lastly, we assessed photobleaching on a confocal microscope using a 640 nm laser with I = 43 kW cm^{-2}, and observed that both SulfoOxazines700 were indeed more resistant (Fig. 1B and G), with the non-deuterated version showing a bit more stability, however, non-significant at any given time point.

Next, we wanted to investigate if **SulfoOxazine700-d10** is compatible in biological settings. We performed a WST-1 assay for cell viability, for which we incubated CHO-K1 cells for 24 hours with 1 μM and 10 μM of either **ATTO700** or

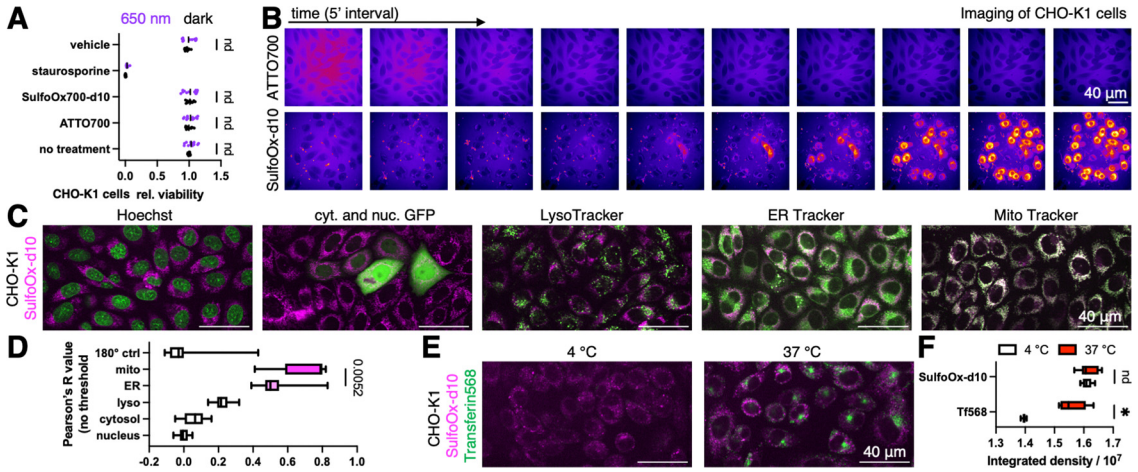

Fig. 2 Live cell application of SulfoOxazine-d10 to label mitochondria. (A) WST-1 assay to assess cell viability of CHO-K1 cells after 1 µM exposure to ATTO700 or SulfoOxazine700-d10 (±light) over night, normalized to non-treated cells in the dark. Scatter dot plot, 2 biological replicates, n = 5–6. (B) Confocal spinning disk imaging of CHO-K1 cells in the presence of either ATTO700 or SulfoOxazine700-d10. λ_{Exc} = 638 nm; λ_{Em} = 700 nm/75 bandpass. 2 biological replicates, >5 ROIs each. (C) Fixed CHO-K1 cells after 45 min treatment with SulfoOxazine700-d10 and respective organellar staining. (D) Co-localization quantification for (C) by Pearson's R value reveals significant mitochondrial accumulation. Unpaired t-test. Min to max box and whiskers. 180° rotated channel served as a control. (E) Uptake assay of SulfoOxazine700-d10 at 4 °C and 37 °C in the presence of fluorescent transferrin568 (for endocytosis) reveals non-active uptake. 10 images. (F) Integrated density quantification for (E). 8 images. Unpaired t-test, $p^* < 0.000001$, nd = not a discovery. Min to max box and whiskers.

SulfoOxazine700-d10 in the dark, or with a 10 minute illumination period using 650 nm of light, before assessing metabolic activity (Fig. 2A and Fig. S1A (ESI†); no treatment, vehicle or 10 µM staurosporine served as controls). We were pleased that under no conditions, except positive control, cell viability was affected. Given the charged nature of the dyes, we aimed to use confocal microscopy to perform shadow imaging of CHO-K1 cells, a technique that is amenable to long-term morphological observations, due to the extracellular replenishment of the dye.[16] We incubated CHO-K1 cells with 1 µM of **ATTO700** or **SulfoOxazine700-d10** and acquired images in 5 minute intervals (Fig. 2B). While we observed some bleaching for **ATTO700**, cellular outlines were identifiable over 45 minutes. Applying **SulfoOxazine700-d10**, however, lead to intracellular signals over the same time period. In order to test for organellar accumulation, we co-incubated with Hoechst (nucleus), transfected with nuclear and cytosolic GFP, LysoTracker, endoplasmic reticulum (ER) tracker or mitochondrial (Mito) Tracker (Fig. 2C). Running Pearson's R value co-localization tests, we confirmed the by eye observation that SulfoOxazine predominantly stains mitochondria (Fig. 2D). To obtain mechanistic information, we performed SulfoOxazine700-d10 uptake in the presence of transferrin568 (by endocytosis) at 4 °C (for blocking endocytosis) and at 37 °C (Fig. 2E), and found, when integrating total channel densities, that our dye enters cells presumably due to passive diffusion and/or aggregation, the mechanisms of which are of ongoing debate.[17] Importantly, **SulfoOxazine700-d10** might serve as a potential non-toxic carrier and/or contrast agent in biological systems.[18] Nevertheless, imaging mitochondria remains a challenge, as these highly dynamic organelles are closely associated with cellular metabolism and function. MitoTracker derivatives are useful, but they sometimes affect mitochondrial function and miss certain mitochondrial populations.[19] **SulfoOxazine700-d10** could represent an alternative for experiments on living cells in the near-infrared window.

Lastly, we were interested in the photophysics of SulfoOxazines in more detail. We did not observe significant pH

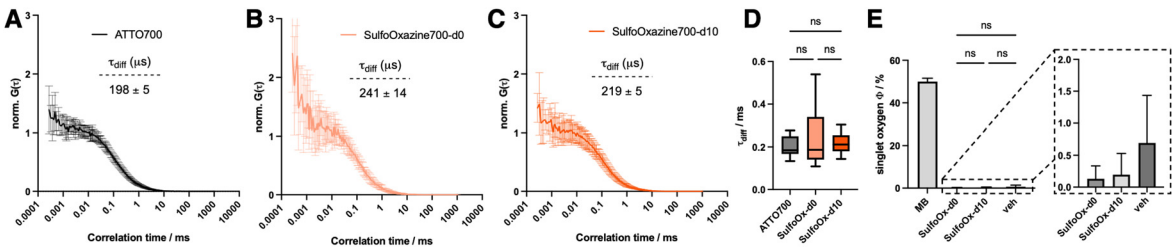

Fig. 3 Single-molecule recordings and singlet oxygen quantum yield of oxazines. Normalized fluorescence correlation spectra of (A) ATTO700, (B) SulfoOxazine700-d0 and (C) SulfoOxazine700-d10. (D) Extracted diffusion times from (A)–(C) between dyes. n = 10; τ_{diff}: n = 8–10. Min to max box and whiskers. λ_{Exc} = 690 nm; λ_{Em} = 740 nm/60 bandpass. (E) Singlet oxygen quantum yields with reference to methylene blue (MB) and compared to vehicle (veh). n = 3. ns = non-significant. one-way ANOVA.

dependence (Fig. S1B, ESI†) and performed fluorescence correlation spectroscopy on 100 pM concentrated samples in buffer (20 mM Tris, 50 mM NaCl, pH = 7.5). **ATTO700**, **SulfoOxazine700-d0** and **SulfoOxazine700-d10** gave clear autocorrelation curves (Fig. 3A–C), which were fit to a single component diffusion model to extract τ-values for diffusion, which remained for all three tested molecules around $\tau_{diffusion} \sim 0.2$ ms (Fig. 3D). Given the small differences in size and molecular weight of the measured species, and the fact that we did not observe large changes in Φ, this was to be expected, and demonstrates that **SulfoOxazine700-d10** might be used as a brighter replacement for **ATTO700**, which has recently been used in different settings, such as DNA-PAINT,[20] as local water sensing molecules,[21] and to probe ligand-receptor interactions.[22] This is also reflected by low singlet oxygen quantum yields (0.2% and 0.1%) for **SulfoOxazine700-d0/d10** (Fig. 3E) *versus* methylene blue. In addition to this, derivatizing **ATTO700** to **SulfoOxazine700-d10** has a minimal impact on its molecular structure and size. With a molecular weight of 517 Da, it is in a similar regime as JF_{690} (458 Da),[1] SiR700 (423 Da)[23] and 2XR-1 (468 Da),[5] which are dimmer ($\varepsilon \times \Phi \sim 12$, 36 and 12, respectively), and have been used for *in vivo* and cellular imaging, respectively. Other available NIR dyes, for which structures are not always available, show a markedly increased size, for instance Alexa Fluor 700 with a $M_w \sim 1300$ Da (ref. 24) or CF700 with a $M_w \sim 2315$ Da (ref. 25). Although the former is reportedly brighter ($\varepsilon \times \Phi \sim 51$), their size may impact their use in dynamic single molecule recordings. Together, our results may play a role in single molecule (sm) imaging approaches, where every photon counts, *e.g.* in smFRET, where a larger extinction coefficient of the acceptor will lead to a larger overlap integral. As such, an increased Förster distance allows measuring longer ranges with a **SulfoOx-700 d10** acceptor, compared to **ATTO700**.

In summary, the deuteration strategy of chromophores was applicable to oxazines to boost brightness, photostability and fluorescence lifetime. Given the interest in near-infrared dyes for better imaging quality in the life sciences due to better tissue penetration of light and less phototoxicity, we highlight **SulfoOxazine700-d10** as a negatively charged dye that is non-cytotoxic and enters cells actively, and might become a superior alternative in single molecule microscopy.

BGF, JS, and KS performed chemical synthesis and characterization, ML and MB photophysical characterization. BGF, MB and JB recorded single molecule spectroscopy. CHO and RB performed cell experiments. BGF, SM and JB conceived and supervised the study. BGF and JB wrote the manuscript with input from all authors. This project has received funding from the European Research Council (ERC) under the European Union's Horizon Europe Framework Programme (deuterON, Grant agreement no. 101042046 to JB) and under the European Union's Horizon 2020 research and innovation program (MultiMotif, grant agreement no. 802209 to SM). Funded by Boehringer Ingelheim Foundation (Exploration Grant to JB). We thank Michael Krauss and Volker Haucke for support (both FMP).

Data availability

The data supporting this article have been included as part of the ESI.†

Conflicts of interest

There are no conflicts to declare.

Notes and references

1 J. B. Grimm, A. N. Tkachuk, L. Xie, H. Choi, B. Mohar, N. Falco, K. Schaefer, R. Patel, Q. Zheng, Z. Liu, J. Lippincott-Schwartz, T. A. Brown and L. D. Lavis, *Nat. Methods*, 2020, **17**, 815–821.
2 N. I. Rubtsova, M. C. Hart, A. D. Arroyo, S. A. Osharovich, B. K. Liebov, J. Miller, M. Yuan, J. M. Cochran, S. Chong, A. G. Yodh, T. M. Busch, E. J. Delikatny, N. Anikeeva and A. V. Popov, *Bioconjug. Chem.*, 2021, **32**, 1852–1863.
3 J. Ast, A. N. Novak, T. Podewin, N. H. F. Fine, B. Jones, A. Tomas, R. Birke, K. Roßmann, B. Mathes, J. Eichhorst, M. Lehmann, A. K. Linnemann, D. J. Hodson and J. Broichhagen, *JACS Au*, 2022, **2**, 1007–1017.
4 X.-X. Zhang, F. Yang, X. Zhao, Q. Wu, L. He, Z. Li, Z. Zhou, T.-B. Ren, X.-B. Zhang and L. Yuan, *Angew. Chem., Int. Ed.*, 2024, **63**, e202410666.
5 W. Wu, K. Yan, Z. He, L. Zhang, Y. Dong, B. Wu, H. Liu, S. Wang and F. Zhang, *J. Am. Chem. Soc.*, 2024, **146**, 11570–11576.
6 C. T. Jackson, S. Jeong, G. F. Dorlhiac and M. P. Landry, *iScience*, 2021, **24**, 102156.
7 M. Trumpp, A. Oliveras, H. Gonschior, J. Ast, D. J. Hodson, P. Knaus, M. Lehmann, M. Birol and J. Broichhagen, *Chem. Commun.*, 2022, **58**, 13724–13727.
8 J. B. Grimm, L. Xie, J. C. Casler, R. Patel, A. N. Tkachuk, N. Falco, H. Choi, J. Lippincott-Schwartz, T. A. Brown, B. S. Glick, Z. Liu and L. D. Lavis, *JACS Au*, 2021, **1**, 690–696.
9 K. Roßmann, K. C. Akkaya, P. Poc, C. Charbonnier, J. Eichhorst, H. Gonschior, A. Valavalkar, N. Wendler, T. Cordes, B. Dietzek-Ivanšić, B. Jones, M. Lehmann and J. Broichhagen, *Chem. Sci.*, 2022, **13**, 8605–8617.
10 H. Janeková, H. C. Friedman, M. Russo, M. Zyberaj, T. Ahmed, A. S. Hua, A. V. Sica, J. R. Caram and P. Šťacko, *Chem. Commun.*, 2024, **60**, 1000–1003.
11 K. Roßmann, A. J. Gonzalez-Hernandez, R. Bhuyan, C. Schattenberg, H. Sun, K. Börjesson, J. Levitz and J. Broichhagen, *Angew. Chem.*, 2024, **63**, e202408300.
12 S. Jung, W.-L. Cheung, S. Li, M. Wang, W. Li, C. Wang, X. Song, G. Wei, Q. Song, S. S. Chen, W. Cai, M. Ng, W. K. Tang and M.-C. Tang, *Nat. Commun.*, 2023, **14**, 6481.
13 S. M. Pauff and S. C. Miller, *Org. Lett.*, 2011, **13**, 6196–6199.
14 **https://www.atto-tec.com/ATTO-700.html**.
15 N. Panchuk-Voloshina, R. P. Haugland, J. Bishop-Stewart, M. K. Bhalgat, P. J. Millard, F. Mao, W.-Y. Leung and R. P. Haugland, *J. Histochem. Cytochem.*, 1999, **47**, 1179–1188.
16 V. V. G. K. Inavalli, V. Puente Muñoz, J. E. Draffin and J. Tønnesen, *Front. Cell. Neurosci.*, 2024, **18**, 1330100.
17 S. Behzadi, V. Serpooshan, W. Tao, M. A. Hamaly, M. Y. Alkawareek, E. C. Dreaden, D. Brown, A. M. Alkilany, O. C. Farokhzad and M. Mahmoudi, *Chem. Soc. Rev.*, 2017, **46**, 4218–4244.
18 A. Albanese and W. C. W. Chan, *ACS Nano*, 2011, **5**, 5478–5489.
19 K. Neikirk, A. G. Marshall, B. Kula, N. Smith, S. LeBlanc and A. Hinton, *Eur. J. Cell Biol.*, 2023, **102**, 151371.
20 N. Gimber, S. Strauss, R. Jungmann and J. Schmoranzer, *Nano Lett.*, 2022, **22**, 2682–2690.
21 J. Maillard, C. A. Rumble and A. Fürstenberg, *J. Phys. Chem. B*, 2021, **125**, 9727–9737.
22 K.-T. Lam, E. L. Taylor, A. J. Thompson, M.-D. Ruepp, M. Lochner, M. J. Martinez and J. A. Brozik, *J. Phys. Chem. B*, 2020, **124**, 7791–7802.
23 Y. Koide, Y. Urano, K. Hanaoka, W. Piao, M. Kusakabe, N. Saito, T. Terai, T. Okabe and T. Nagano, *J. Am. Chem. Soc.*, 2012, **134**, 5029–5031.
24 **https://www.thermofisher.com/order/catalog/product/A20010**.
25 **https://biotium.com/technology/cf-dyes/nir-cf-dyes/**.